

# Reactions of Bis(chalcogenolato) Complexes $[(\eta^5\text{-C}_5\text{Me}_5)\text{Ir}(\text{CO})(\text{ETol})_2]$ (E = Se, S; Tol = *p*-Tolyl) with $[\text{Pt}(\text{PPh}_3)_3]$ . Formation of Tri- or Dinuclear Mixed-Metal Complexes with Bridging Chalcogenido or Chalcogenolato Ligands

Takafumi Nakagawa, Hidetake Seino, and Yasushi Mizobe\*

*Institute of Industrial Science, The University of Tokyo, Komaba, Meguro-ku, Tokyo 153-8505, Japan*

*Received December 10, 2009*

Treatment of  $[\text{Cp}^*\text{Ir}(\text{CO})(\text{SeTol})_2]$  ( $\text{Cp}^* = \eta^5\text{-C}_5\text{Me}_5$ , Tol = *p*-tolyl) with 2 equiv of  $[\text{Pt}(\text{PPh}_3)_3]$  in toluene at reflux resulted in the insertion of Pt(PPh<sub>3</sub>) groups into Se–Tol bonds to give the triangular cluster with capped Se ligands  $[\text{Cp}^*\text{Ir}(\mu_3\text{-Se})_2\{\text{PtTol}(\text{PPh}_3)_2\}_2]$  (**5**). By stirring under CO atmosphere, **5** in solution was readily converted to  $[\text{Cp}^*\text{Ir}(\text{CO})(\mu_3\text{-Se})_2\{\text{PtTol}(\text{PPh}_3)_2\}_2]$  (**2b**), which returned to **5** in toluene at reflux. On the other hand, reaction of  $[\text{Cp}^*\text{Ir}(\text{CO})(\text{STol})_2]$  with an equimolar amount of  $[\text{Pt}(\text{PPh}_3)_3]$  afforded the thiolato-bridged dinuclear complex  $[\text{Cp}^*\text{Ir}(\text{CO})(\mu\text{-STol})\text{Pt}(\text{STol})(\text{PPh}_3)]$  (**6**) through the insertion of the Pt center into the Ir–S bond, and that with 2 equiv of  $[\text{Pt}(\text{PPh}_3)_3]$  in toluene at reflux led to the incorporation of the second Pt fragment to the core of **6** to give the thiolato-bridged triangular cluster  $[\text{Cp}^*\text{Ir}\{\text{Pt}(\text{PPh}_3)_2(\mu_2\text{-CO})(\mu_2\text{-STol})_2\}_2]$  (**7**). An X-ray diffraction study has been carried out to determine the detailed structures of **2b**, **5**, **6**, and  $[\text{Cp}^*\text{Ir}\{\text{Pt}(\text{PPh}_3)_2(\mu_2\text{-CO})(\mu_2\text{-SPh})_2\}_2]$ , which is the SPh analogue of **7**.

## Introduction

In a previous paper,<sup>1</sup> we have reported that organic ditelluride TolTeTeTol (Tol = *p*-tolyl) reacts smoothly with  $[\text{Cp}^*\text{Ir}(\text{CO})_2]$  ( $\text{Cp}^* = \eta^5\text{-C}_5\text{Me}_5$ ) to give bis(tellurolato) complex  $[\text{Cp}^*\text{Ir}(\text{CO})(\text{TeTol})_2]$  (**1a**), and then **1a** is treated with 2 equiv of  $[\text{Pt}(\text{PPh}_3)_3]$  or  $[\text{Pd}(\text{PPh}_3)_4]$  at room temperature to afford bis( $\mu$ -tellurido) clusters  $[\text{Cp}^*\text{Ir}(\text{CO})(\mu_3\text{-Te})_2\{\text{MTol}(\text{PPh}_3)_2\}_2]$  (M = Pt (**2a**), Pd (**3a**)) via the insertion of the Pt(PPh<sub>3</sub>) or Pd(PPh<sub>3</sub>) groups into the Te–Tol bonds (Scheme 1). From the reaction of **1a** with an equimolar amount of  $[\text{Pt}(\text{PPh}_3)_3]$ , the dinuclear complex containing both  $\mu$ -tellurido and  $\mu$ -tellurolato ligands  $[\text{Cp}^*\text{Ir}(\text{CO})(\mu\text{-Te})(\mu\text{-TeTol})\text{PtTol}(\text{PPh}_3)]$  (**4**) was isolated as the intermediate stage toward **2a**. These findings have demonstrated that the easily available, organic ditelluride TolTeTeTol can be used as the convenient tellurium source soluble in organic media to derivatize the tellurido complexes. It has also been emphasized that the chemistry of the heavier chalcogen complexes,<sup>2</sup> especially tellurium complexes, is still poorly advanced in contrast to that of the complexes with sulfur ligands.

To clarify the difference in reactivities between the complexes with the tellurium and the lighter chalcogen ligands, we have extended the study on the reactions of the bis(tellurolato)

complex **1a** with  $[\text{Pt}(\text{PPh}_3)_3]$  to those of bis(selenolato) and bis(thiolato) analogues  $[\text{Cp}^*\text{Ir}(\text{CO})(\text{ETol})_2]$  (E = Se (**1b**), S (**1c**)). As expected, it has been revealed that the reaction courses are sharply affected by the nature of the chalcogen atoms. In this paper we describe the results of these reactions and the structures of new tri- and dinuclear Ir–Pt complexes having bridging selenium and sulfur ligands obtained here. Multimetallic complexes with sulfur and heavier chalcogen ligands are continuously attracting much attention because of their relevance to the active sites of certain biological and industrial catalysts.<sup>2,3</sup>

## Results and Discussion

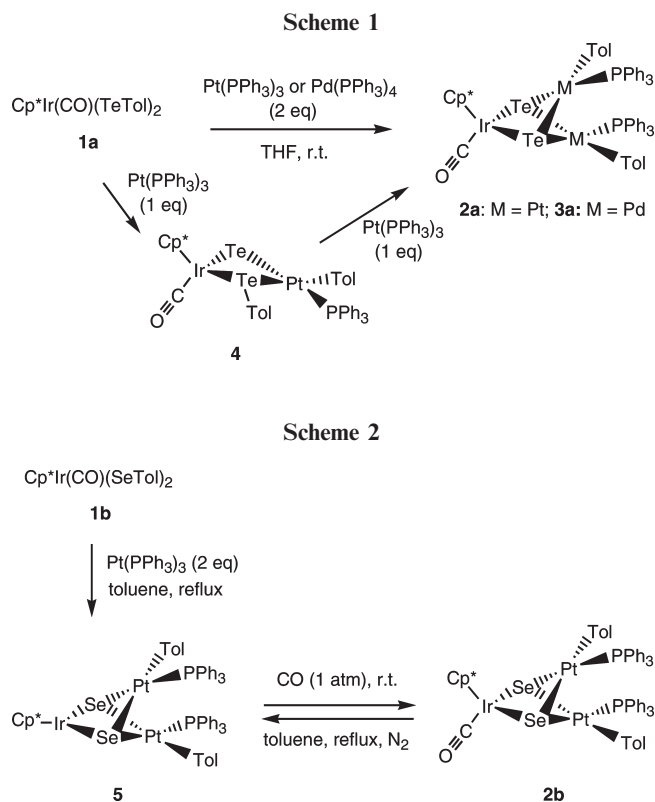
**Reaction of 1b with  $[\text{Pt}(\text{PPh}_3)_3]$ .** The reaction of **1b** with  $[\text{Pt}(\text{PPh}_3)_3]$  did take place in THF and toluene even at room temperature. However, the NMR spectra showed the formation of complicated mixtures, and no characterizable products were isolated therefrom. On the other hand, under more drastic conditions the reaction system becomes simple. Thus, when the mixture of **1b** and 2 equiv of  $[\text{Pt}(\text{PPh}_3)_3]$  in toluene was heated to reflux for 3 h, the trinuclear bis(selenido) cluster  $[\text{Cp}^*\text{Ir}(\mu_3\text{-Se})_2\{\text{PtTol}(\text{PPh}_3)_2\}_2]$  (**5**) was isolated from the reaction mixture in 33% yield as green crystals (Scheme 2).

\*Corresponding author. E-mail: ymizobe@iis.u-tokyo.ac.jp.

(1) Nakagawa, T.; Seino, H.; Nagao, S.; Mizobe, Y. *Angew. Chem., Int. Ed.* **2006**, *45*, 7758.

(2) (a) Gimeno, M. C. In *Handbook of Chalcogen Chemistry*; Derillanova, F. A., Ed.; RSC Publishing: Cambridge, UK, 2009; pp 33–80. (b) Singh, A. J.; Sharma, S. *Coord. Chem. Rev.* **2000**, *209*, 49. (c) Parkin, G. *Prog. Inorg. Chem.* **1998**, *47*, 1. (d) Trnka, T. M.; Parkin, G. *Polyhedron* **1997**, *16*, 1031. (e) Arnold, J. *Prog. Inorg. Chem.* **1995**, *43*, 353.

(3) (a) Rao, P. V.; Holm, R. H. *Chem. Rev.* **2004**, *104*, 527. (b) Lee, S. C.; Holm, R. H. *Chem. Rev.* **2004**, *104*, 1135. (c) Llusar, R.; Uriel, S. *Eur. J. Inorg. Chem.* **2003**, 1271. (d) Degroot, M. W.; Corrigan, J. F. In *Comprehensive Coordination Chemistry II*; McCleverty, J. A.; Meyer, T. J., Eds.; Elsevier: New York, 2004; Vol. 7, pp 57–123. (e) Brorson, M.; King, J. D.; Kiriakidou, K.; Prestopino, F.; Nordlander, E. In *Metal Clusters in Chemistry*; Braunstein, P.; Oro, L. A.; Raitby, P. R., Eds.; Wiley-VCH: Weinheim, Germany, 1999; pp 725–741. (f) Blower, P. J.; Dilworth, J. R. *Coord. Chem. Rev.* **1987**, *76*, 121.



Insertion of Pt into Se–Tol bonds resulted in the formation of the  $\text{IrPt}_2(\mu_3\text{-Se})_2$  core analogous to **2a**, but the CO ligand was lost from the Ir site. As for the reaction of **1b** with 1 equiv of  $[\text{Pt}(\text{PPh}_3)_3]$ , no tractable products were obtained even after refluxing in toluene.

For the formation of **5**, dissociation of CO is presumed to take place owing to the drastic conditions employed. Thus, when the reaction mixture containing crude **5** in toluene was stirred under CO (1 atm) at room temperature, the color of the solution changed rapidly from green to orange. From the resultant solution,  $[\text{Cp}^*\text{Ir}(\text{CO})(\mu_3\text{-Se})_2\{\text{PtTol}(\text{PPh}_3)_2\}]$  (**2b**) was isolated in 38% yield based on **1b** as red crystals. It has been confirmed independently by recording the NMR spectra of the reaction mixtures that **5** is quantitatively converted into **2b** by stirring its THF solution under CO (1 atm) at room temperature, while **2b**, when dissolved in toluene under  $\text{N}_2$  and heated at reflux, is transformed back to **5** exclusively (Scheme 2). It is to be noted that in the case of the tellurido cluster **2a** the Ir–CO bond is intact even after heating in toluene at reflux.

**Structures of 2b and 5.** Single-crystal X-ray analysis has disclosed the detailed structures for **2b** and **5**, whose ORTEP drawings are shown in Figures 1 and 2, respectively. Selected interatomic distances and angles are listed in Table 1. Crystals of **2b** contained two crystallographically independent molecules, whose structures are essentially the same.

Cluster **2b**, consisting of a 50-electron  $\text{IrPt}_2$  core, is isostructural with **2a**. Thus, the Ir(III) center, with three-legged piano-stool geometry, is connected with two square-planar Pt(II) centers by two  $\mu_3\text{-Se}$  ligands. Two  $\text{PPh}_3$  ligands have an anti disposition with respect to the  $\text{Pt}\cdots\text{Pt}$  vector, and there are no bonding interactions between metals. However, interatomic distances in the core of **2b** (Ir $\cdots$ Pt: 3.5308(7)–3.6211(8) Å; Pt $\cdots$ Pt: 3.0201(8) and 3.1068(9) Å) are all much shorter than those in **2a** (Ir $\cdots$ Pt: 3.8054(5)–3.8588(5) Å; Pt $\cdots$ Pt: 3.1543(4) and 3.2523(7) Å), and hence the former is

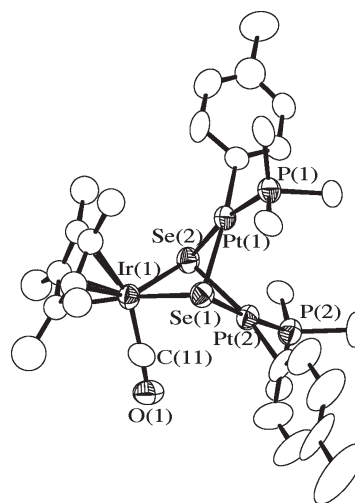


**Figure 1.** ORTEP drawing of **2b** (50% probability level). One of the two crystallographically independent molecules is depicted. For clarity, all hydrogen atoms are omitted and only the ipso-C atoms of the Ph groups are shown for  $\text{PPh}_3$  ligands.

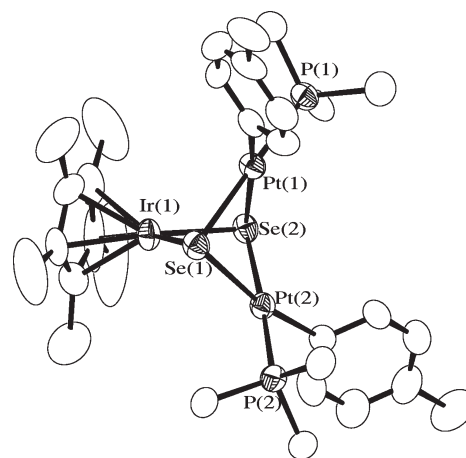


**Figure 2.** ORTEP drawing of **5** (50% probability level). For clarity, all hydrogen atoms are omitted and only the ipso-C atoms of the Ph groups are shown for  $\text{PPh}_3$  ligands.

**Table 1.** Selected Interatomic Distances (Å) and Angles (deg) in **2b** and **5**

	<b>2b</b> (molecule 1)	<b>2b</b> (molecule 2)	<b>5</b>
(a) Interatomic Distances			
Ir $\cdots$ Pt(1)	3.6062(8)	3.6211(8)	3.0931(7)
Ir $\cdots$ Pt(2)	3.5308(7)	3.5514(7)	3.1961(6)
Pt(1) $\cdots$ Pt(2)	3.1068(9)	3.0201(8)	3.2691(6)
Ir–Se(1)	2.528(2)	2.521(1)	2.422(1)
Ir–Se(2)	2.508(1)	2.510(2)	2.416(1)
Pt(1)–Se(1)	2.537(2)	2.493(2)	2.466(1)
Pt(1)–Se(2)	2.481(2)	2.517(2)	2.498(1)
Pt(2)–Se(1)	2.478(1)	2.541(1)	2.517(1)
Pt(2)–Se(2)	2.557(2)	2.490(2)	2.449(1)
(b) Interatomic Angles			
Se(1)–Ir–Se(2)	75.87(4)	76.05(5)	85.04(4)
Se(1)–Ir–C(11)	92.6(4)	93.1(5)	
Se(2)–Ir–C(11)	92.7(4)	91.0(5)	
Se(1)–Pt(1)–Se(2)	76.18(5)	76.42(5)	82.41(4)
Se(1)–Pt(2)–Se(2)	75.87(4)	76.04(4)	82.36(4)

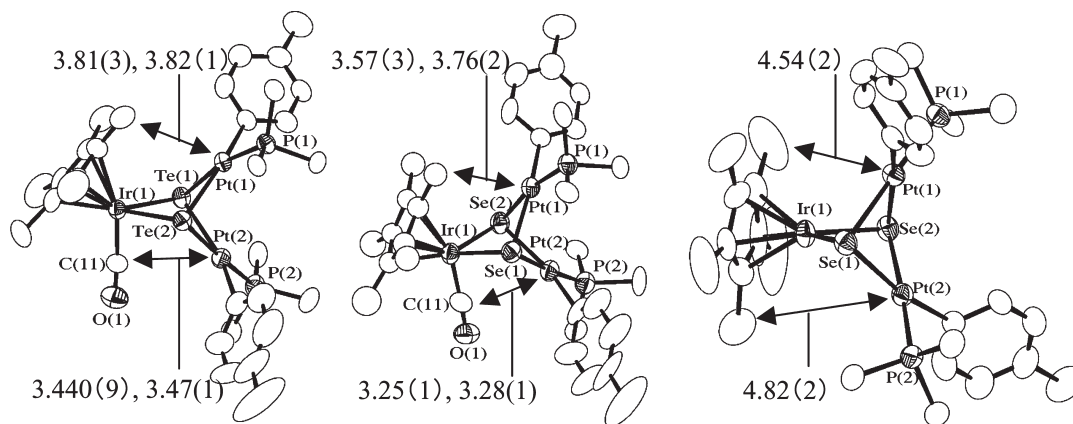
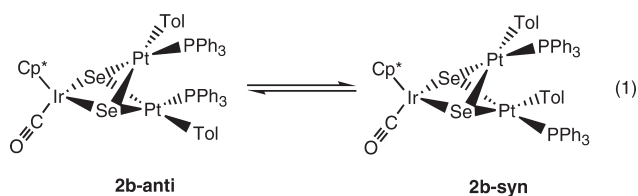


**Figure 3.** Comparison of selected interatomic distances (Å) related to the steric crowding in **2a**, **2b**, and **5** (from left to right). Values of two crystallographically independent molecules are given for **2a** and **2b**.

apparently sterically more congested than the latter. This may result in the more severe steric repulsion between Cp\* and the PtTol(PPh<sub>3</sub>) fragment as well as that between CO and the PtTol(PPh<sub>3</sub>) scaffold, as shown in Figure 3, which presumably accounts for the finding that the CO in **2b** is more dissociative. The  $\nu(\text{CO})$  values at 1983 and 1979 cm<sup>-1</sup> in **2b** and **2a**, respectively, differ only slightly, suggesting that the electronic factor is essentially negligible with respect to the difference in the dissociating ability of CO ligands between these two.

The 48-electron cluster **5** consists of the Ir(III) center with a two-legged geometry together with two square-planar Pt(II) centers. The Ir···Pt distances at 3.0931(7) and 3.1961(6) Å are significantly shorter than those in **2b**, but nevertheless, owing to the change in the geometry around Ir caused by the loss of CO, steric repulsion apparently diminishes to a great extent, as depicted in Figure 3.

The <sup>1</sup>H and <sup>31</sup>P{<sup>1</sup>H} NMR spectra have disclosed that **2b** exists as a mixture of two isomers in a ratio of 9:1 in C<sub>6</sub>D<sub>6</sub> solution at room temperature. This feature can be interpreted in terms of the equilibrium between the X-ray analyzed anti isomer and the syn isomer (eq 1), which was also observed for **2a** but in a ratio of 4:1. We propose that the latter isomer is less stable due to the larger repulsion between two PPh<sub>3</sub> ligands. Similar isomerization also occurs for **5** in solution, where the anti:syn ratio is ca. 10 in C<sub>6</sub>D<sub>6</sub>.



The related triangular Ir(III)<sub>2</sub>Pt(II) core with two capped Se ligands [(Cp\*Ir)<sub>2</sub>(PtCl<sub>2</sub>)(μ<sub>3</sub>-Se)<sub>2</sub>] was reported previously,<sup>4</sup> while the Pt(II)<sub>3</sub>(μ<sub>3</sub>-Se)<sub>2</sub> cores were fully characterized for [Pt(PPh<sub>3</sub>)<sub>2</sub>(μ<sub>3</sub>-Se)<sub>2</sub>][Pt(cod)]<sub>2</sub>[PF<sub>6</sub>]<sub>2</sub> and [Pt(cod)(μ<sub>3</sub>-Se)<sub>2</sub>][Pt(PPh<sub>3</sub>)<sub>2</sub>]<sub>2</sub>[PF<sub>6</sub>]<sub>2</sub>.<sup>5</sup>

**Reactions of 1c with [Pt(PPh<sub>3</sub>)<sub>3</sub>].** Reaction of the bis(thiolato) complex **1c** with 1 equiv of [Pt(PPh<sub>3</sub>)<sub>3</sub>] proceeded cleanly in

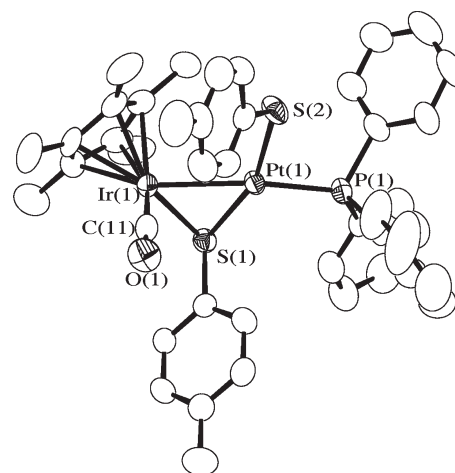
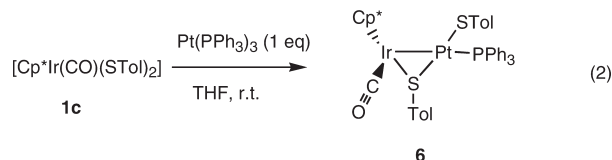


**Figure 4.** ORTEP drawing of **6** (50% probability level). Hydrogen atoms are omitted for clarity.

THF at room temperature to give the dinuclear complex [Cp\*Ir(CO)(μ-STol)Pt(STol)(PPh<sub>3</sub>)] (**6**) in moderate yield (eq 2). Complex **6** is thermally stable, and its structure is retained even after heating in toluene at reflux. In this reaction, insertion of Pt occurs at one Ir–S bond in **1c** to afford an Ir–Pt–STol array and the Ir–Pt bond is bridged by the other STol ligand. Complex **6** has been characterized by X-ray diffraction (Figure 4, Table 2).



Complex **6** has a formal Ir(II)Pt(I) core with an Ir–Pt bond of 2.6918(3) Å. If this bonding interaction is ignored, the Ir and Pt centers have two-legged piano-stool and severely distorted T-shaped structures, respectively. Around Pt, the Pt–μ-S(1) distance at 2.270(1) Å is significantly shorter than the terminal thiolato Pt–S(2) bond length (2.327(1) Å). Complex **6** shows a characteristic  $\nu(\text{CO})$  band at 1951 cm<sup>-1</sup>, which is much lower than 1991 cm<sup>-1</sup> observed for the parent **1c**. This might be interpreted by the difference in the formal oxidation state of Ir centers, viz., +2 in **6** and +3 in **1c**. The

(4) Nagao, S.; Seino, H.; Hidai, M.; Mizobe, Y. *J. Organomet. Chem.* **2003**, *669*, 124.

(5) Teo, J. S. L.; Vittal, J. J.; Henderson, W.; Hor, T. S. A. *Inorg. Chem.* **2002**, *41*, 1194.

**Table 2. Selected Bond Distances (Å) and Angles (deg) in 6 and 7'**

6			
(a) Interatomic Distances			
Ir–Pt	2.6918(3)	Ir–S(1)	2.318(1)
Pt–S(1)	2.270(1)	Pt–S(2)	2.327(1)
(b) Interatomic Angles			
S(1)–Ir–C(11)	94.1(2)	S(1)–Pt–S(2)	159.01(5)
S(1)–Pt–P(1)	110.84(5)	S(2)–Pt–P(1)	89.43(5)
7' <sup>a</sup>			
(a) Interatomic Distances			
Ir–Pt(1)	2.7043(5)	Ir–Pt(2)	2.6718(5)
Pt(1)–Pt(2)	2.8061(4)		
Ir–C(11)	2.09(1)	Ir–S(1)	2.252(2)
Pt(1)–S(1)	2.307(3)	Pt(1)–S(2)	2.349(2)
Pt(2)–S(2)	2.418(2)	Pt(2)–C(11)	1.94(1)
(b) Interatomic Angles			
Pt(1)–Ir–Pt(2)	62.92(1)	Ir–Pt(1)–Pt(2)	57.97(1)
Ir–Pt(2)–Pt(1)	59.10(1)	S(1)–Ir–C(11)	98.5(2)
S(1)–Pt(1)–S(2)	144.43(7)	S(1)–Pt(1)–P(1)	108.81(8)
S(2)–Pt(1)–P(1)	106.76(6)	S(2)–Pt(2)–P(2)	111.54(7)
S(2)–Pt(2)–C(11)	143.2(3)	P(2)–Pt(2)–C(11)	105.2(3)

<sup>a</sup>Data for one of the two disordered molecules with larger occupancy.

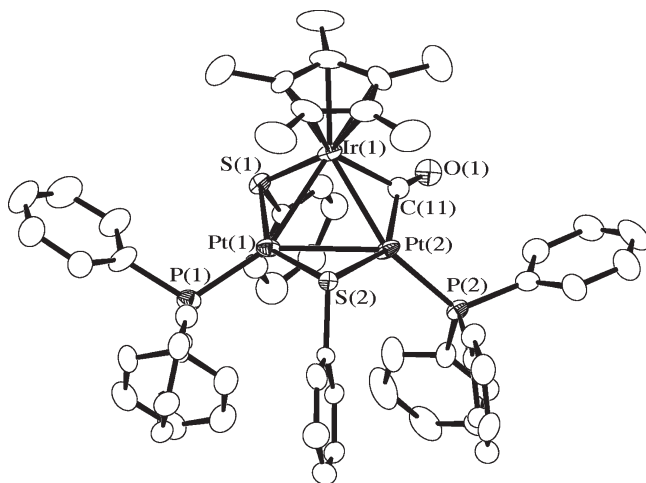
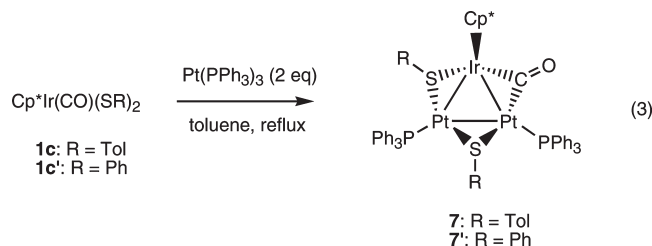


**Figure 5.** ORTEP drawing of 7' (50% probability level). Hydrogen atoms are omitted for clarity.

dinuclear Ir(II) complex  $[\{\text{Cp}^*\text{Ir}(\text{CO})\}_2(\mu\text{-S})]$  has been reported to exhibit a  $\nu(\text{CO})$  band at  $1929\text{ cm}^{-1}$ .<sup>6</sup>

Dinuclear cores supported by only one  $\kappa^1$  S atom ligand are still rare, which include, for example,  $[\text{Pd}(\text{C}_6\text{F}_5)(\text{phen})-(\mu\text{-SC}_6\text{F}_5)\text{Pt}(\text{C}_6\text{F}_5)(\text{dppe})]$ , in which the Pd and Pt centers without a direct bonding interaction are connected by a  $\text{SC}_6\text{F}_5$  ligand.<sup>7</sup> The Ir and Mo centers without an Ir–Mo bond in  $[\{\text{Cp}^*\text{IrH}(\text{PPh}_3)\}_2(\mu\text{-S})\{\text{MoCp}^*\text{Cl}(\text{NO})\}]$  are combined by a sulfido ligand,<sup>8</sup> while the Ir–Ir single bonds in  $[\{\text{Cp}^*\text{Ir}(\text{CO})\}_2(\mu\text{-S})]$  and  $[\{\text{Cp}^*\text{Ir}(\text{PMe}_3)\}_2(\mu\text{-S})\{\text{Ir}(\text{PPh}_3)(\text{NO})\}]$  are supported by a bridging S ligand.<sup>6,9</sup>

When **1c** was reacted with 2 equiv of  $[\text{Pt}(\text{PPh}_3)_3]$  in toluene at room temperature, the reaction mixture contained only **6** and Pt– $\text{PPh}_3$  complexes. In contrast, when this mixture was heated to reflux for 5 h,  $[\text{Cp}^*\text{Ir}\{\text{Pt}(\text{PPh}_3)\}_2(\mu_2\text{-CO})(\mu_2\text{-STol})_2]$  (**7**) was obtained (eq 3), where the second  $\{\text{Pt}(\text{PPh}_3)\}$  fragment is incorporated with concurrent binding to the C atom of the CO ligand as well as the S atom of the terminal STol ligand in **6**, affording the triangular IrPt<sub>2</sub> core with one  $\mu_2\text{-CO}$  and two  $\mu_2\text{-STol}$  ligands. Unfortunately, **7** was not isolable as an analytically pure form and was characterized only spectroscopically. On the other hand, analogous treatment of the SPh congener  $[\text{Cp}^*\text{Ir}(\text{CO})(\text{SPh})_2]$  (**1c'**) with 2 equiv of  $[\text{Pt}(\text{PPh}_3)_3]$  led to the isolation of single crystals of  $[\text{Cp}^*\text{Ir}\{\text{Pt}(\text{PPh}_3)\}_2(\mu_2\text{-CO})(\mu_2\text{-SPh})_2]$  (**7'**) (eq 3), whose structure could be determined in a well-defined manner. The ORTEP drawing is shown in Figure 5, and selected metrical parameters are listed in Table 2.



Cluster **7'** has a triangular IrPt<sub>2</sub> core with a 46-electron count, where the Ir–Pt distances at 2.7043(5) and 2.6718(5) Å as well as the Pt–Pt separation of 2.8061(4) Å indicate the presence of metal–metal single bonds. One Ir–Pt bond is bridged by the CO ligand, while the other two edges are coordinated with  $\mu_2\text{-SPh}$  groups. Two P atoms of  $\text{PPh}_3$  ligands are almost coplanar with the IrPt<sub>2</sub> triangle, whereas the Cp\* ligand and S(2) atom are directed to one side of the IrPt<sub>2</sub> plane and the S(1) and C(11) atoms are situated at the opposite side of this plane. The  $\nu(\text{CO})$  band observed at  $1731\text{ cm}^{-1}$  in the IR spectrum is consistent with its  $\mu_2$  bridging mode. The triangular Pt<sub>3</sub> core with  $\mu_2$ -thiolato bridges was crystallographically characterized for, for example, the Pt(II) cluster without Pt–Pt bonds,  $[\text{Pt}_3\{\mu_2\text{-S-}o\text{-C}_6\text{H}_4\text{-N}=\text{CH}-(\pi\text{-C}_5\text{H}_5)\text{Fe}(\pi\text{-C}_5\text{H}_5)\}_3\text{-}\kappa^3\text{-S,N,C}]$ ,<sup>10</sup> while that with  $\mu_2\text{-CO}$  ligands was presumed for, for example, Pt(0) clusters without Pt–Pt bonds,  $[\{\text{Pt}(\text{PR}_3)\}_3(\mu_2\text{-CO})_3]$ .<sup>11</sup>

## Conclusions

The reaction of the selenolato complex **1b** with  $[\text{Pt}(\text{PPh}_3)_3]$  proceeded similarly to that previously reported for the telluroolato complex **1a**, yielding the IrPt<sub>2</sub>( $\mu_3\text{-Se}$ )<sub>2</sub> core via the insertion of Pt into the Se–Tol bonds. However, more drastic conditions were required for **1b**. In contrast, the thiolato analogue **1c** is amenable to the insertion of Pt into the Ir–S bond to give first the Ir( $\mu\text{-STol}$ )Pt–STol complex and then the triangular IrPt<sub>2</sub>( $\mu_2\text{-STol}$ )<sub>2</sub> cluster. These findings are consistent with the findings previously reported for the reactions of Ph<sub>2</sub>E (E = Te, Se, S) with  $[\text{Pt}(\text{PEt}_3)_3]$ , where the oxidative addition of Ph–E bonds proceeds most readily

(6) Jones, W. D.; Chin, R. M. *J. Am. Chem. Soc.* **1994**, *116*, 198.

(7) Usón, R.; Usón, M. A.; Herrero, S.; Rello, L. *Inorg. Chem.* **1998**, *37*, 4473.

(8) Arashiba, K.; Matsukawa, S.; Tanabe, Y.; Kuwata, S.; Ishii, Y. *Inorg. Chem. Commun.* **2008**, *11*, 587.

(9) Hattori, T.; Matsukawa, S.; Kuwata, S.; Ishii, Y.; Hidai, M. *Chem. Commun.* **2003**, 510.

(10) Nagasawa, I.; Kawamoto, T.; Kuma, H.; Kushi, Y. *Chem. Lett.* **1996**, 921.

(11) (a) Browning, C. S.; Farrar, D. H.; Gukathasan, R. R.; Morris, S. A. *Organometallics* **1985**, *4*, 1750. (b) Ros, R.; Facchin, G.; Tassan, A.; Roulet, R.; Laurency, G.; Lukacs, F. *J. Cluster Sci.* **2001**, *12*, 99.

for E = Te and becomes more difficult for E = Se and S in this order.<sup>12</sup> It has also been demonstrated that the reactions of the cluster  $[\text{Os}_3(\text{CO})_{10}(\text{MeCN})_2]$  with furan and its heavier chalcogen analogues  $\text{C}_4\text{H}_4\text{E}$  (E = O, S, Se, Te) lead to the compounds formed by C–H bond cleavage for E = O and S or by C–E cleavage for E = Se and Te.<sup>13</sup> These data and our result clearly present that the reactivity of chalcogen–carbon bonds toward transition metal complexes increases stepwise in the order S, Se, and Te.

It should be mentioned finally that the reactions of **1b** and **1c** with  $[\text{Pd}(\text{PPh}_3)_4]$  were also carried out. The spectroscopic evidence supported that  $[\text{Cp}^*\text{Ir}(\mu_3\text{-Se})_2\{\text{PdTol}(\text{PPh}_3)_2\}]$  and  $[\text{Cp}^*\text{Ir}\{\text{Pd}(\text{PPh}_3)_2\}_2(\mu_2\text{-CO})(\mu_2\text{-STol})_2]$  were produced similarly. However, none of these could be isolated either in analytically pure form or as single crystals for X-ray diffraction (see Supporting Information).

## Experimental Section

**General Procedures.** All manipulations were carried out under  $\text{N}_2$  using standard Schlenk techniques. Solvents were dried by common methods and distilled under  $\text{N}_2$  before use. Complex  $[\text{Cp}^*\text{Ir}(\text{CO})(\text{SPh})_2]$  was prepared according to the literature method,<sup>14</sup> and related **1b** and **1c** were synthesized by essentially the same but slightly modified procedure. Complex  $[\text{Pt}(\text{PPh}_3)_3]$  was obtained as described previously.<sup>15</sup>

IR and NMR spectra were obtained by a JASCO FT-IR 420 or a JEOL alpha-400 spectrometer, respectively. For the  $^1\text{H}$  NMR data, the signals due to  $\text{PPh}_3$  are omitted. The  $^{31}\text{P}\{^1\text{H}\}$  NMR spectra containing both  $^{195}\text{Pt}$  and  $^{77}\text{Se}$  satellites were analyzed by line-shape simulation using gNMR software.<sup>16</sup> Where two  $J_{\text{Pt-P}}$  values are given for one  $^{31}\text{P}$  signal, the smaller one corresponds to the long-range coupling constant. Elemental analyses were done with a Perkin-Elmer 2400 series II CHN analyzer.

**Preparation of 5.** A mixture of **1b** (71 mg, 0.10 mmol) and  $[\text{Pt}(\text{PPh}_3)_3]$  (204 mg, 0.207 mmol) in toluene (10 mL) was refluxed for 3 h. After cooling to room temperature, the resultant dark green solution was concentrated, and then hexane was added to precipitate **5** as green crystals (55 mg, 33% yield). Anal. Calcd for  $\text{C}_{60}\text{H}_{59}\text{P}_2\text{Se}_2\text{IrPt}_2$ : C, 45.54; H, 3.76. Found: C, 45.39; H, 3.61. For **5-anti**:  $^1\text{H}$  NMR ( $\text{C}_6\text{D}_6$ ):  $\delta$  1.54 (s, 15H, Cp\*), 2.19 (s, 6H, Me), 6.70, 7.31 (d,  $J = 8.0$  Hz, 4H each,  $\text{C}_6\text{H}_4$ ).  $^{31}\text{P}\{^1\text{H}\}$  NMR ( $\text{C}_6\text{D}_6$ ):  $\delta$  17.0 (m with  $^{195}\text{Pt}$  and  $^{77}\text{Se}$  satellites,  $^1J_{\text{Pt-P}} = 4230$  Hz,  $^2J_{\text{Se(trans)-P}} = 68$  Hz); other coupling constants ( $< 6$  Hz) could not be assigned unambiguously because of a highly complicated  $\text{PPtPtSeSe}$  spin system. For **5-syn**:  $^1\text{H}$  NMR ( $\text{C}_6\text{D}_6$ ):  $\delta$  1.57 (s, 15H, Cp\*), 2.16 (s, 6H, Me), 6.70, 7.31 ( $\text{C}_6\text{H}_4$ , overlapping with those of **5-anti**).  $^{31}\text{P}\{^1\text{H}\}$  NMR ( $\text{C}_6\text{D}_6$ ):  $\delta$  16.6 (s with  $^{195}\text{Pt}$  satellites,  $^1J_{\text{Pt-P}} = 4235$  Hz); the other satellite peaks were too weak to be assigned. The ratio of **5-anti**:**5-syn** was ca. 10.

**Preparation of 2b.** The reaction mixture containing **5** was prepared as described above and then thoroughly degassed. The reaction vessel was filled with CO (1 atm), and the mixture was stirred overnight at room temperature. The resulting orange solution was dried in vacuo, and the residue was crystallized from benzene–hexane. The yield of **2b**·0.25 $\text{C}_6\text{H}_{14}$  as red crystals was 62 mg (38% based on **1b**). Anal. Calcd for  $\text{C}_{62.5}\text{H}_{62.5}\text{OP}_2\text{Se}_2\text{IrPt}_2$ : C, 46.00; H, 3.86. Found: C, 46.37; H, 3.53. For

**2b-anti**:  $^1\text{H}$  NMR ( $\text{C}_6\text{D}_6$ ):  $\delta$  1.61 (s, 15H, Cp\*), 2.12, 2.20 (s, 3H each, Me), 6.70, 6.82, 7.47, 7.58 (d,  $J = 8.0$  Hz, 2H each,  $\text{C}_6\text{H}_4$ ).  $^{31}\text{P}\{^1\text{H}\}$  NMR ( $\text{C}_6\text{D}_6$ ):  $\delta$  11.1 (d with  $^{195}\text{Pt}$  and  $^{77}\text{Se}$  satellites,  $J_{\text{P-P}} = 5$  Hz,  $J_{\text{Pt-P}} = 3920$  and 8 Hz,  $J_{\text{Se-P}} = 85$  and  $\sim 20$  Hz), 12.8 (d with  $^{195}\text{Pt}$  and  $^{77}\text{Se}$  satellites,  $J_{\text{P-P}} = 5$  Hz,  $J_{\text{Pt-P}} = 3830$  and 8 Hz,  $J_{\text{Se-P}} = 76$  and  $\sim 20$  Hz). For **2b-syn**:  $^1\text{H}$  NMR ( $\text{C}_6\text{D}_6$ ):  $\delta$  1.63 (s, 15H, Cp\*); the signals due to Tol are overlapping with those of **2b-anti**.  $^{31}\text{P}\{^1\text{H}\}$  NMR ( $\text{C}_6\text{D}_6$ ):  $\delta$  9.5 (d,  $J_{\text{P-P}} = 7$  Hz), 10.2 (d,  $J_{\text{P-P}} = 7$  Hz); the  $^{195}\text{Pt}$  and  $^{77}\text{Se}$  satellites were too weak to be assigned. The ratio of **2b-anti**:**2b-syn** was ca. 9.

**Preparation of 6.** Into a THF solution (5 mL) of **1c** (295 mg, 0.490 mmol) was added  $[\text{Pt}(\text{PPh}_3)_3]$  (485 mg, 0.494 mmol), and the mixture was stirred at room temperature for 2 days. Addition of hexane to the concentrated product solution gave **6** as red crystals (305 mg, 58% yield). Anal. Calcd for  $\text{C}_{43}\text{H}_{44}\text{OPS}_2\text{IrPt}$ : C, 48.76; H, 4.19. Found: C, 49.20; H, 4.00. IR (KBr):  $\nu(\text{CO})$ ,  $1951\text{ cm}^{-1}$ .  $^1\text{H}$  NMR ( $\text{C}_6\text{D}_6$ ):  $\delta$  1.81 (d,  $J = 1.6$  Hz, 15H, Cp\*), 1.87, 2.13 (s, 3H each, Me), 6.60, 6.90, 7.58, 7.93 (d,  $J = 8.0$  Hz, 2H each,  $\text{C}_6\text{H}_4$ ).  $^{31}\text{P}\{^1\text{H}\}$  NMR ( $\text{C}_6\text{D}_6$ ):  $\delta$  15.3 (s with  $^{195}\text{Pt}$  satellites,  $J_{\text{Pt-P}} = 3735$  Hz).

**Preparation of 7.** A mixture of **1c** (59 mg, 0.10 mmol) and  $[\text{Pt}(\text{PPh}_3)_3]$  (200 mg, 0.204 mmol) in toluene (5 mL) was stirred at room temperature. The NMR spectra of the reaction mixture indicated the presence of only **6** and Pt- $\text{PPh}_3$  complexes. Then the mixture was heated to reflux for 5 h, and after cooling to room temperature the resultant dark green solution was evaporated to dryness in vacuo. The spectral data of the residue are diagnostic of the formation of **7**, but analytically pure crystals were not available in spite of the repeated purification. IR (KBr):  $\nu(\text{CO})$ ,  $1731\text{ cm}^{-1}$ .  $^1\text{H}$  NMR ( $\text{C}_6\text{D}_6$ ):  $\delta$  2.07 (d,  $J_{\text{H-P}} = 0.8$  Hz, 15H, Cp\*), 1.82, 1.97 (s, 3H each, Me), 6.07, 6.69, 7.58, 7.93 (d,  $J = 8.0$  Hz, 2H each,  $\text{C}_6\text{H}_4$ ).  $^{31}\text{P}\{^1\text{H}\}$  NMR ( $\text{C}_6\text{D}_6$ ):  $\delta$  8.7 (d with  $^{195}\text{Pt}$  satellites,  $J_{\text{P-P}} = 32$  Hz,  $J_{\text{Pt-P}} = 4510$  and 315 Hz), 40.4 (d with  $^{195}\text{Pt}$  satellites,  $J_{\text{P-P}} = 32$  Hz,  $J_{\text{Pt-P}} = 6030$  and 160 Hz).

**Preparation of 7'.** A mixture containing  $[\text{Cp}^*\text{Ir}(\text{CO})(\text{SPh})_2]$  (59 mg, 0.10 mol) and  $[\text{Pt}(\text{PPh}_3)_3]$  (200 mg, 0.204 mmol) in toluene (5 mL) was refluxed for 5 h. After cooling to room temperature, the resulting dark green solution was dried in vacuo. The residue was washed with MeOH and then crystallized from benzene–hexane. The yield of **7'** as green crystals was 16 mg (11%). Anal. Calcd for  $\text{C}_{59}\text{H}_{55}\text{OP}_2\text{S}_2\text{IrPt}_2$ : C, 47.61; H, 3.72. Found: C, 47.64; H, 3.83. IR (KBr):  $\nu(\text{CO})$ ,  $1731\text{ cm}^{-1}$ .  $^1\text{H}$  NMR ( $\text{C}_6\text{D}_6$ ):  $\delta$  2.06 (d,  $J_{\text{H-P}} = 0.8$  Hz, 15H, Cp\*), 6.30 (t,  $J = 6.0$  Hz, 2H, SPh), 6.44 (t,  $J = 6.0$  Hz, 1H, SPh), 6.84 (m, 4H, SPh), 7.43 (m, 3H, SPh).  $^{31}\text{P}\{^1\text{H}\}$  NMR ( $\text{C}_6\text{D}_6$ ):  $\delta$  8.6 (d with  $^{195}\text{Pt}$  satellites,  $J_{\text{P-P}} = 32$  Hz,  $J_{\text{Pt-P}} = 4480$  and 320 Hz), 40.5 (d with  $^{195}\text{Pt}$  satellites,  $J_{\text{P-P}} = 32$  Hz,  $J_{\text{Pt-P}} = 6020$  and 120 Hz).

**X-ray Crystallography.** Single crystals of **2b**·0.25 $\text{C}_6\text{H}_{14}$ , **5**, **6** (sealed in glass capillaries under argon), and **7'** (coated with mineral oil) were mounted on a Rigaku Mercury-CCD diffractometer equipped with a graphite-monochromatized Mo  $\text{K}\alpha$  source. Diffraction studies were done at 20 °C for **2b**·0.25 $\text{C}_6\text{H}_{14}$ , **5**, and **6** and at  $-160$  °C for **7'** by using CrystalClear program package,<sup>17</sup> whose details are listed in Table 3. All diffraction data were corrected for absorption.

Structure solution and refinements were conducted by using the CrystalStructure program package.<sup>18</sup> The positions of non-hydrogen atoms were determined by Patterson methods (PATTY)<sup>19</sup>

(12) Han, L.-B.; Choi, N.; Tanaka, M. *J. Am. Chem. Soc.* **1997**, *119*, 1795.

(13) Arce, A. J.; Deeming, A. J.; De Sanctis, Y.; Machado, R.; Manzur, J.; Rivas, C. *J. Chem. Soc., Chem. Commun.* **1990**, 1568.

(14) Herberhold, M.; Jin, G.-X.; Rheingold, A. L. *J. Organomet. Chem.* **1998**, *570*, 241.

(15) Ugo, R.; Cariati, F.; La Monica, G. *Inorg. Synth.* **1968**, *11*, 105.

(16) gNMR: Program for Simulation of One-Dimensional NMR Spectra; Adept Scientific: Amor Way, U.K., 1995–1999.

(17) CrystalClear 1.3.5; Rigaku Corporation, 1999. *CrystalClear Software User's Guide*; Molecular Structure Corporation, 2000. Pflugrath J. W. *Acta Crystallogr. D* **1999**, *55*, 1718.

(18) CrystalStructure 3.8.0: Crystal Structure Analysis Package; Rigaku and Rigaku/MS, 2000–2006. Carruthers, J. R.; Rollett, J. S.; Betteridge, P. W.; Kinna, D.; Pearce, L.; Larsen, A.; Gabe, E. *CRYSTALS Issue 11*; Chemical Crystallography Laboratory: Oxford, U.K., 1999.

(19) Beurskens, P. T.; Admiraal, G.; Beurskens, G.; Bosman, W. P.; Garcia-Granda, S.; Gould, R. O.; Smits, J. M. M.; Smykall, C. *PATTY, The DIRDIF Program System*; Technical Report of the Crystallography Laboratory; University of Nijmegen: Nijmegen, The Netherlands, 1992.

Table 3. Crystal Data for **2b**·0.25C<sub>6</sub>H<sub>14</sub>, **5**, **6**, and **7'**

	<b>2b</b> ·0.25C <sub>6</sub> H <sub>14</sub>	<b>5</b>	<b>6</b>	<b>7'</b>
formula	C <sub>62.5</sub> H <sub>62.5</sub> IrOP <sub>2</sub> Pt <sub>2</sub> Se <sub>2</sub>	C <sub>60</sub> H <sub>59</sub> IrP <sub>2</sub> Pt <sub>2</sub> Se <sub>2</sub>	C <sub>43</sub> H <sub>44</sub> IrOPPtS <sub>2</sub>	C <sub>62</sub> H <sub>58</sub> IrOP <sub>2</sub> Pt <sub>2</sub> S <sub>2</sub>
fw	1631.95	1582.39	1059.22	1527.61
cryst syst	triclinic	triclinic	triclinic	monoclinic
space group	<i>P</i> $\bar{1}$ (No. 2)	<i>P</i> $\bar{1}$ (No. 2)	<i>P</i> $\bar{1}$ (No. 2)	<i>P</i> 2 <sub>1</sub> / <i>n</i> (No. 14)
<i>a</i> , Å	14.872(4)	10.729(3)	9.187(2)	11.2868(8)
<i>b</i> , Å	18.127(4)	13.475(4)	10.727(2)	40.900(2)
<i>c</i> , Å	22.248(5)	19.873(6)	20.867(3)	12.8571(8)
$\alpha$ , deg	96.423(3)	80.076(10)	90.904(2)	90
$\beta$ , deg	103.352(4)	80.078(10)	91.274(2)	114.5349(9)
$\gamma$ , deg	95.387(3)	78.17(1)	102.718(3)	90
<i>V</i> , Å <sup>3</sup>	5754(2)	2742(2)	2005.1(5)	5399.4(6)
<i>Z</i>	4	2	2	4
<i>d</i> <sub>calcd.</sub> , g cm <sup>-3</sup>	1.88	1.92	1.75	1.88
cryst size, mm <sup>3</sup>	0.20 × 0.13 × 0.13	0.20 × 0.20 × 0.20	0.30 × 0.25 × 0.10	0.40 × 0.40 × 0.20
no. of unique reflns	25 998 ( <i>R</i> <sub>int</sub> = 0.070)	12 051 ( <i>R</i> <sub>int</sub> = 0.046)	8782 ( <i>R</i> <sub>int</sub> = 0.029)	12 125 ( <i>R</i> <sub>int</sub> = 0.073)
no. of data with <i>I</i> > 2σ( <i>I</i> )	12 142	7523	6575	10 940
no. of variables	1329	663	486	675
transmn factor	0.159–0.331	0.094–0.168	0.262–0.498	0.137–0.210
<i>R</i> <sub>1</sub> <sup>a</sup>	0.064	0.056	0.030	0.055
<i>wR</i> <sub>2</sub> <sup>b</sup>	0.193	0.158	0.103	0.144
GOF <sup>c</sup>	1.050	1.006	1.014	1.357

<sup>a</sup>  $R_1 = \sum ||F_o| - |F_c|| / \sum |F_o|$  (*I* > 2σ(*I*)). <sup>b</sup>  $wR_2 = [\sum (w(F_o^2 - F_c^2)^2) / \sum w(F_o^2)^2]^{1/2}$  (all data). <sup>c</sup> GOF =  $[\sum w(|F_o| - |F_c|)^2 / \{(\text{no. observed}) - (\text{no. variables})\}]^{1/2}$ .

and subsequent Fourier synthesis (DIRDIF99),<sup>20</sup> which were refined with anisotropic thermal parameters by full-matrix least-squares techniques. Hydrogen atoms were placed at the calculated positions and included at the final stages of the refinements with fixed parameters.

**Acknowledgment.** This work was supported by a Grant-in-Aid for Scientific Research on Priority Areas (No.

18065005, “Chemistry of Concerto Catalysis”) and in part by the Global COE Program “Chemistry Innovation through Cooperation of Science and Engineering” from the Ministry of Education, Culture, Sports, Science and Technology, Japan. JSPS Grant-in-Aid for Fellows (20-6569) is also appreciated (T.N.).

(20) Beurskens, P. T.; Admiraal, G.; Beurskens, G.; Bosman, W. P.; de Gelder, R.; Israel, R.; Smits, J. M. M. *The DIRDIF-99 Program System*; Technical Report of the Crystallography Laboratory; University of Nijmegen: Nijmegen, The Netherlands, 1999.

**Supporting Information Available:** Details of X-ray crystallographic data in CIF format for **2b**·0.25C<sub>6</sub>H<sub>14</sub>, **5**, **6**, and **7'** and additional experimental procedures. This material is available free of charge via the Internet at <http://pubs.acs.org>.